Published in final edited form as:
Exp Neurol. 2013 November ; 249: . doi:10.1016/j.expneurol.2013.08.015.

Sympathetic denervation of peri-infarct myocardium requires the p75 neurotrophin receptor

Christina U. Lorentz[a], **Diana C. Parrish**[a], **Eric N. Alston**[a], **Michael J. Pellegrino**[a], **William R. Woodward**[b], **Barbara L. Hempstead**[c], and **Beth A. Habecker**[a]

[a]Department of Physiology and Pharmacology, Oregon Health and Science University, 3181 SW Sam Jackson Park Rd., Portland, Oregon 97239, USA

[b]Department of Neurology, Oregon Health and Science University, 3181 SW Sam Jackson Park Rd., Portland, Oregon 97239, USA

[c]Division of Hematology and Medical Oncology, Department of Medicine, Weill Cornell Medical College, 1300 York Avenue, New York, NY 10065, USA

Abstract

Development of cardiac sympathetic heterogeneity after myocardial infarction contributes to ventricular arrhythmias and sudden cardiac death. Regions of sympathetic hyperinnervation and denervation appear in the viable myocardium beyond the infarcted area. While elevated nerve growth factor (NGF) is implicated in sympathetic hyperinnervation, the mechanisms underlying denervation are unknown. Recent studies show that selective activation of the p75 neurotrophin receptor ($P75^{NTR}$) in sympathetic neurons causes axon degeneration. We used mice that lack $p75^{NTR}$ to test the hypothesis that activation of $p75^{NTR}$ causes peri-infarct sympathetic denervation after cardiac ischemia-reperfusion. Wild type hearts exhibited sympathetic denervation adjacent to the infarct 24 hours and 3 days after ischemia-reperfusion, but no peri-infarct sympathetic denervation occurred in *$p75^{NTR}$−/−* mice. Sympathetic hyperinnervation was found in the distal peri-infarct myocardium in both genotypes 3 days after MI, and hyperinnervation was increased in the *$p75^{NTR}$−/−* mice. By 7 days after ischemia-reperfusion, cardiac sympathetic innervation density returned back to sham-operated levels in both genotypes, indicating that axonal pruning did not require $p75^{NTR}$. Prior studies revealed that proNGF is elevated in the damaged left ventricle after ischemia-reperfusion, as is mRNA encoding brain derived neurotrophic factor (BDNF). ProNGF and BDNF preferentially bind $p75^{NTR}$ rather than TrkA on sympathetic neurons. Immunohistochemistry using *Bdnf-HA* mice confirmed the presence of BDNF or proBDNF in the infarct after ischemia-reperfusion. Thus, at least two $p75^{NTR}$ ligands are elevated in the left ventricle after ischemia-reperfusion where they may stimulate $p75^{NTR}$-dependent denervation of peri-infarct myocardium. In contrast, NGF-induced sympathetic hyperinnervation in the distal peri-infarct ventricle is attenuated by $p75^{NTR}$.

Address correspondence to: Beth A. Habecker, Ph.D., Dept. of Physiology & Pharmacology, L334, Oregon Health and Science University, 3181 SW Sam Jackson Park Rd., Portland, OR 97239, TEL: (503) 494-0497, FAX: (503) 494-4352, habecker@ohsu.edu.

Keywords

ischemia-reperfusion; axon degeneration; Brain Derived Neurotrophic Factor; regeneration; pruning

Introduction

Myocardial infarction (MI) leads to increased risk of ventricular arrhythmias and sudden cardiac death (Solomon et al., 2005), and altered sympathetic transmission in the heart is a major contributor to the development of these arrhythmias (2000). Several types of changes have been characterized in cardiac sympathetic nerves after MI including denervation of viable peri-infarct myocardium (Barber et al., 1983; Inoue and Zipes, 1988; Li et al., 2004; Minardo et al., 1988; Stanton et al., 1989), areas of nerve sprouting and hyperinnervation (Cao et al., 2000; Hasan et al., 2006; Oh et al., 2006; Zhou et al., 2004), and regional changes in neurotransmitter and peptide production (Alston et al., 2011; Li et al., 2004; Parrish et al., 2009b). Heterogeneity of sympathetic transmission and subsequent electrical remodeling of cardiac myocytes is thought to be a major contributor to arrhythmias in humans (Rubart and Zipes, 2005). Two recent studies examined sympathetic innervation in patients shortly after reperfusion by imaging uptake of the NE transporter substrate iodine-123 meta-iodobenzylguanidine (123I-MIBG). Patients then received implanted cardioverter defibrillators (ICDs), which allowed for long-term monitoring of cardiac rhythm. Both studies concluded that a larger area of sympathetic denervation after MI correlated with a higher risk for arrhythmias at later time points (Boogers et al., 2010; Nishisato et al., 2010).

Given the clinical importance of peri-infarct denervation, we were interested in understanding what caused the loss of sympathetic axons in viable myocardium. This was particularly puzzling given that nerve growth factor (NGF) is increased in the heart after MI (Abe et al., 1997; Hasan et al., 2006; Hiltunen et al., 2001; Meloni et al., 2010; Zhou et al., 2004). NGF stimulates sympathetic axon growth into the heart through activation of the TrkA receptor tyrosine kinase (Crowley et al., 1994; Glebova and Ginty, 2004; Smeyne et al., 1994), and increasing cardiac NGF causes sympathetic hyperinnervation (Cao et al., 2000; Hassankhani et al., 1995). One potential explanation for denervation comes from our recent observation that proNGF, the uncleaved precursor to mature NGF, is elevated in mouse and human heart after MI (Siao et al., 2012). Previous studies of NGF expression did not distinguish between proNGF and mature NGF, which bind to different receptors and elicit different biological actions. ProNGF binds a heteromeric receptor complex of the p75 neurotrophin receptor ($p75^{NTR}$) and sortilin (Nykjaer et al., 2004), or the sortilin family member, SorCS2 (Siao et al, 2012), through which it stimulates neuronal process retraction (Al Shawi et al., 2007; Deinhardt et al., 2011) or neuronal cell death (Nykjaer et al., 2004). A second potential explanation for peri-infarct denervation comes from the transient induction of brain-derived neurotrophic factor (BDNF) mRNA at the border of the infarct and intact tissue (Hiltunen et al., 2001). BDNF also binds $p75^{NTR}$ on sympathetic neurons, inhibiting sympathetic outgrowth and stimulating axon degeneration (Kohn et al., 1999; Krizsan-Agbas et al., 2003; Singh et al., 2008).

We hypothesized that proNGF and BDNF produced in the heart after MI caused the pathological sympathetic denervation of peri-infarct myocardium via $p75^{NTR}$. Here we provide evidence that BDNF protein is present in the heart after MI, and peri-infarct denervation requires $p75^{NTR}$. Thus, our data suggest that peri-infarct denervation after myocardial infarction, which is pathological in humans, is stimulated by $p75^{NTR}$.

Methods

Animals and Experimental Group

Wildtype C57BL/6J and *p75*$^{NTR-/-}$ mice (B6.129S4-Ngfr^{tm1Jae}/J) (Lee et al., 1992) were obtained from Jackson Laboratories. Homozygous *Bdnf-HA* mice in which the endogenous *Bdnf* coding region was replaced with the murine *Bdnf* sequence fused to a C-terminal hemagglutinin (HA) epitope tag were generated as described by Yang et al. (Yang et al., 2009). Mice were kept on a 12h:12h- light dark cycle with ad libitum access to food and water. Age and gender-matched male and female mice between 12–18 weeks old were used for all experiments. The experimental groups used were sham-operated animals and animals that underwent ischemia-reperfusion surgery. A minimum of four animals was assigned to each group for each experiment, and tissue was processed together for each type of analysis. All procedures were approved by the OHSU Institutional Animal Care and Use Committee and comply with the Guide for the Care and Use of Laboratory Animals published by the National Academies Press (8th edition).

Ischemia-Reperfusion Surgery

Anesthesia was induced with 4% inhaled isoflurane and maintained with 2% isoflurane. Mice were then intubated and mechanically ventilated. Core body temperature was monitored with a rectal probe and maintained at 37°C and two-lead ECG was monitored throughout the surgery using a PowerLab data acquisition system. A left thoracotomy was performed in the 4th intercostal space and the pericardium was opened. The left anterior descending coronary artery (LAD) was reversibly ligated with a 8-0 suture for 30 minutes and then reperfused by release of the ligature. Occlusion was confirmed with ST segment elevation, regional cyanosis, and wall motion abnormalities. Reperfusion was confirmed by return of color to the myocardium distal to the ligation and disappearance of ST elevation. The suture remained within the wound for identification of the ligature site, and the chest and skin were closed in layers. After surgery, animals were returned to individual cages and given regular food and water for 24h, 3 days or 7 days before euthanasia and tissue harvest. Buprenex (0.1 mg/kg) was administered as needed to ensure the animals were comfortable following surgery. All surgical procedures were performed under aseptic conditions. Sham animals underwent the procedure described above except for the LAD ligation.

Immunohistochemistry

All sections were incubated with $NaBH_4$ and $CuSO_4$ as described previously (Lorentz et al., 2010) in order to decrease autofluorescence. Tyrosine Hydroxylase (TH) immunohistochemistry was performed as described previously (Lorentz et al., 2010), using rabbit anti-TH (1:300, Chemicon) and AlexaFluor 488-conjugated rabbit IgG-specific antibody (1:300, Molecular Probes). Tissue from *Bdnf-HA* mice was fixed for 2h in 3% paraformaldehyde rinsed in PBS, cryoprotected in 30% sucrose overnight and 10 μm transverse sections were thaw-mounted onto charged slides. For HA immunohistochemistry and HA/Mac2 double label, sections were blocked in 5% B.S.A/0.1% Triton X-100 in PBS for 1 h followed by blocking with AvidinD blocking buffer (Vector Laboratories) for 15 min. Slides were briefly rinsed with PBS and blocked with Biotin solution (Vector Laboratories) for 15 min. Slides were rinsed again with PBS and incubated with rabbit anti-HA (1:500, Sigma), with or without rat anti-MAC2 (1:500, Accurate Scientific), overnight at 4°C. Slides were then rinsed in PBS and incubated with biotinylated goat anti-rabbit (1:400, Jackson ImmunoResearch), with or without anti-rat AlexaFluor 488, for 1h at room temperature. Slides were washed with PBS and incubated with Cy3-streptavidin (1:800, Jackson ImmunoResearch) for 45 min. Slides were rinsed with PBS, coverslipped and visualized by fluorescence microscopy. For HA/Ly-6B.2 double label, sections were blocked in 5% B.S.A/0.3% Triton X-100/5% goat serum in PBS for 1.5 h, and then

incubated overnight at 4°C with rabbit anti-HA (1:50, Sigma) and rat anti-Ly-6B.2 (1:50, AbD Serotec). Slides were then rinsed in PBS, incubated with species-specific secondary antibodies for 1h at room temperature, rinsed again in PBS, coverslipped, and visualized by fluorescence microscopy.

Innervation Density Analysis

Immunohistochemical staining was visualized on a Zeiss (Axiophot II) fluorescent microscope with the 20X objective. Photos were taken of 11 fields of view (A–K) from each section (Fig. 1A). Four sections approximately 150 μm apart were analyzed from each heart. Each picture occupied an area of 710 μm × 530 μm, which was defined as one field of view. Pictures A and B were taken in the right ventricle. Picture C was taken at the border between the right ventricle and the left ventricle and each successive picture (D–J) was directly adjacent to the previous picture without overlap. Picture K was taken from the interventricular septum. $P75^{NTR-/-}$ mice lack subendocardial sympathetic innervation (Lorentz et al., 2010). Therefore, all pictures from the left ventricle were confined to the subepicardial layer of muscle. Innervation density was determined by threshold discrimination (ImageJ) as previously described (Lorentz et al., 2010) and each image was quantified by two independent observers and averaged together.

Pictures containing any infarcted myocardium were considered infarct. Peri-infarct 1 was defined as the field of view adjacent to the infarct and peri-infarct 2 was defined as the field of view adjacent to peri-infarct 1 (530 μm from the edge of the infarct). Analyzing these three regions allowed us to control for variable positioning of the infarct within the individual animals. Innervation density from the fields of view that corresponded to proximal and distal peri-infarct regions were averaged together and were compared to the corresponding region from sham-operated animals (regions E, D and H respectively, Fig. 1A, E). Because the infarct usually occupied more than one field of view, one representative infarct picture from each section was chosen and averaged across the four sections from one heart.

In vitro TH enzyme activity assay

Superior cervical ganglia (SCG) from neonatal rats were dissociated and grown in C2 medium supplemented with 10 ng/mL nerve growth factor (NGF, BD Bioscience), and 3% fetal bovine serum (ATCC) as previously described (Pellegrino et al., 2011) and maintained in a humidified 5% CO_2 incubator at 37°C. Sympathetic neurons were grown in 24-well plates pre-coated with 100 μg/mL poly-L-lysine (Sigma) and 10 μg/mL collagen (BD bioscience), and non-neuronal cells were eliminated by treating the cultures with the anti-mitotic agent, cytosine arabinoside (Ara C, 1 μM, Sigma) for 2 days. Neurons were then treated for 0, 2, or 20 hours with 100 ng/ml NGF prior to analysis of TH activity.

Cultures (60,000 neurons/well) were homogenized in 150 μL of 5 mM Tris-acetate buffer (pH 6.0) containing 0.1% Triton X-100, protease inhibitor cocktail (Roche) and sodium orthovanadate (1 mM). TH enzyme activity was determined by measuring the rate of L-DOPA production from L-tyrosine under standardized conditions (Acheson et al., 1984; Shi et al., 2012). A 60 μL aliquot of the homogenate was combined with an equal volume of reaction buffer and assayed for TH activity under the following conditions: 120 mM Tris-acetate buffer (pH 6.0), 3 mM 6-methyl-5, 6, 7, 8 tetrahydropterin HCl (BH4), 10 mM 2-mercaptoethanol, catalase (200,000 U/mL), 100 μM L-tyrosine, and the internal standard, 1.0 μM 3,4-dihydroxybenzylamine (DHBA). The reaction mixtures were incubated at 37°C. Aliquots (20 μL) of the reaction mixture were removed at regular intervals (every 4 min) and added to 1 mL of a chilled solution containing 0.5 M Tris-acetate buffer (pH 8.0), 0.1 M EDTA, and 15 mg of alumina to stop the reaction. The L-DOPA and DHBA were purified

by an alumina extraction procedure and measured by HPLC using electrochemical detection as described previously (Li et al., 2004). Levels of TH protein were assessed by western blot analysis and were found not to differ significantly between replicates within a treatment group (n=4) or between treatment groups. We therefore express TH activity as the amount of L-DOPA produced per culture (i.e. 60,000 neurons) with respect to time.

HPLC Analysis of NE

NE levels were measured by HPLC with electrochemical detection as described previously (Parrish et al., 2009a). Below the site of LAD occlusion the left and right ventricles (LV, RV) were separated and processed individually for NE analysis. Heart tissue was homogenized in perchloric acid (0.1 M) containing 1.0 μM of the internal standard dihydroxybenzylamine to correct for sample recovery. Catecholamines were purified by alumina extraction before analysis by HPLC. Detection limits were ~0.05 pmol with recoveries from the alumina extraction >60%.

Immunoblot Analysis

Cells were washed with ice-cold PBS and lysed at 4°C in homogenization buffer as described above. Lysates were fractionated on SDS-polyacrylamide gels and transferred to nitrocellulose membranes. Blots were incubated in 3% low fat milk in Tris-buffered saline (pH 7.4) containing 0.1% tween-20 at room temperature. Membranes were subsequently incubated at 4°C overnight with rabbit anti-TH (1:5000, Millipore), rabbit anti-pTH Ser31 (1:1000, Cell Signaling), or rabbit anti-pERK1/2 (Cell Signaling #9101). Immunoblots were incubated with horseradish peroxidase HRP-conjugated secondary antibody and immune complexes were visualized by chemiluminescence (Super Signal Dura, Pierce).

Statistics

Student's t-test was used for a single comparison between two groups (WT vs. p75NTR). One-way ANOVA with a Neuman-Keuls post-test was used to compare across multiple groups within the same genotype. Two-way ANOVA with a Bonferroni post-test was used to compare across genotypes and treatment groups.

Results

To quantitate sympathetic innervation after MI, we initially averaged each field of view (A–K) across four sections from each heart in order to obtain an unbiased analysis of sympathetic innervation density. Table 1 shows innervation density from WT hearts 3 days and 7 days after ischemia-reperfusion surgery. However, the position of the infarct in the left ventricle was not the same in all four sections analyzed from one heart (Fig. 1B), nor was it the same between animals due to anatomical variability of LAD morphology and surgical variability (Scherrer-Crosbie et al., 1997). Therefore, the data were re-analyzed segregating the infarct from peri-infarct myocardium. Once the infarct was identified for each section (Fig. 1C), three regions of the left ventricle emerged as areas of interest: the infarct, the proximal peri-infarct region directly adjacent to the infarct (peri-infarct 1 or P1) and distal peri-infarct region (peri-infarct 2 or P2; 450 μm from the infarct) (Fig. 1D).

Sympathetic innervation density was similar in sham- operated wildtype (WT) and $p75^{NTR-/-}$ mice in regions corresponding to the infarct and peri-infarct in mice undergoing cardiac ischemia-reperfusion (Fig. 1E, 3C–D). Sympathetic innervation densities of sham-operated hearts collected 3 days and 7 days after surgery were identical and were pooled into one sham group.

To test the hypothesis that cardiac sympathetic denervation occurs through $p75^{NTR}$ we analyzed sympathetic fiber density in wild type (WT) and $p75^{NTR-/-}$ mice 24 hours, 3 days and 7 days after ischemia-reperfusion surgery. The infarct was significantly denervated in both genotypes by 24 hours (Fig. 2), and this sympathetic denervation persisted through 3 and 7 days after surgery (Fig. 2). The infarct remained substantially denervated 7 days after ischemia- reperfusion but occasional TH+ fibers were observed within the infarct of mice from both genotypes (data not shown).

Innervation density in the peri-infarct ventricle was dynamic. Twenty-four hours after MI sympathetic innervation density decreased significantly in the proximal peri-infarct region of WT mice (Fig. 3A, C, E). This did not occur in the $p75^{NTR-/-}$ mice (Fig. 3B, D, F). No change in sympathetic innervation density was detected in the distal peri-infarct region of WT hearts 24 hours after ischemia-reperfusion (Fig. 3A, G) but significant sympathetic hyperinnervation was present in the distal peri-infarct region of $p75^{NTR-/-}$ mice (Fig. 3B, H).

Three days after MI significant sympathetic denervation was observed in the proximal peri-infarct region in WT mice (Fig. 4A, C, E) but no decrease in innervation density was observed in the same region from $p75^{NTR-/-}$ mice (Fig. 4B, D, F). At the same time, significant hyperinnervation was observed in the distal peri-infarct region of WT mice (Fig. 4A, G) and $p75^{NTR-/-}$ mice (Fig. 4B, H). Sympathetic hyperinnervation was significantly greater in the $p75^{NTR-/-}$ distal peri-infarct region compared to WT ($p< 0.01$, two-way ANOVA with Bonferroni post-test).

Surprisingly, sympathetic innervation density was elevated in the $p75^{NTR-/-}$ right ventricle 3 days after MI compared to WT (Sham fiber density: WT 1.96±0.1, $p75^{NTR-/-}$ 1.9±0.3 and MI fiber density: WT 2.2±0.4, $p75^{NTR-/-}$ 3.8±0.5*; *$p<0.05$, mean±sem, n=6–8), but NE content was similar to WT right ventricle (WT 1.8±0.2 pmol/mg, $p75^{NTR-/-}$ 1.6±0.1 pmol/mg, mean±sem, n=5). TH and NE are both elevated in control $p75^{NTR-/-}$ hearts compared to WT (Habecker et al., 2008; Lorentz et al., 2010), and NGF is thought stimulate TH activity by increasing TH content (Naujoks et al., 1982; Otten et al., 1977; Thoenen et al., 1971). We recently found, however, that inflammatory cytokines that suppress TH content in sympathetic neurons (Yamamori et al., 1989) also stimulate activity of the remaining TH enzyme (Shi et al., 2012). Therefore, we asked if NGF regulated TH activity in addition to its effect on TH levels. Treatment with high levels of NGF (100 ng/ml) for 2 or 20 hours did not alter TH activity, as assessed by measuring the kinetics of L-DOPA production (Figure 5A). Consistent with the lack of affect on TH activity, phosphorylation of TH on serine 31 was not changed by chronic treatment (2 or 20hrs, data not shown) or acute treatment with NGF (Figure 5B, C).

One week after ischemia-reperfusion surgery, there were no significant differences in peri-infarct innervation density compared to surgical sham animals. Sympathetic innervation in the WT proximal peri-infarct region continued to trend low, although it was not significantly different than sham (Fig. 6A). In addition, the sympathetic hyperinnervation observed 3 days after myocardial infarction was no longer present in either genotype (Fig. 6A–B, RV data not shown). Despite this, the distribution of the sympathetic fibers was altered compared to sham-operated animals. Instead of the even distribution of sympathetic fibers throughout the myocardium seen in the sham operated animals, sympathetic fibers were unevenly distributed, with areas of denervation and adjacent areas containing clusters of TH+ fibers (Fig. 6C).

The loss of sympathetic nerve fibers adjacent to the infarct required $p75^{NTR}$, suggesting that ischemia-reperfusion induced expression of a $p75^{NTR}$ ligand that stimulated axon

degeneration outside of the infarct. Potential $p75^{NTR}$ ligands in the heart include proNGF which is elevated in the left ventricle 24 hours and 3 days after reperfusion (Siao et al., 2012) and proBDNF or mature BDNF (Hiltunen et al., 2001). BDNF mRNA is transiently elevated at the peri-infarct border zone after ischemia-reperfusion (Hiltunen et al., 2001), and we asked if that led to the production of BDNF protein. In order to localize BDNF expression within the ventricle we used homozygous *Bdnf-HA* mice (Yang et al., 2009). Immunohistochemistry to detect HA-tagged BDNF revealed increased HA immunoreactivity 24 hours after MI compared to sham operated control animals (Fig. 7). The HA staining was localized predominantly to the infarct. Interestingly, HA immunohistochemistry revealed punctate staining, raising the possibility that one source of BDNF was infiltrating immune cells. To determine if this was the case, we stained sections for the HA tag as well as a marker to identify neutrophils or macrophages. Many HA-positive cells co-stained for the neutrophil marker Ly-6B.2 (Fig. 7C), but no HA-immunoreactive cells co-stained for the macrophage marker Mac2 (Fig. 7D). Similar results were obtained with other macrophage markers (not shown).

Discussion

Previous studies examining innervation density in the heart after myocardial infarction have analyzed only regions of sympathetic hyperinnervation or denervation, excluding large areas from analysis (Hasan et al., 2006; Oh et al., 2006; Zhou et al., 2004). Here we carried out a systematic analysis of innervation across the ventricle after ischemia-reperfusion. We found that analyzing the same region at different levels of the ventricle was not the best way to assess changes in cardiac nerves. Although infarct size is similar in $p75^{-/-}$ and WT hearts 24 hrs after MI (Lorentz et al., 2011), the shape of the infarct changes across the different levels. Thus, we identified the infarct and analyzed innervation density based on proximity to the infarct within that section. This method revealed significant sympathetic denervation adjacent to the infarct, combined with significant hyperinnervation in the distal peri-infarct myocardium. This is the first study to analyze total innervation density, and characterize both hyperinnervation and hypoinnervation in the same heart after myocardial infarction.

We found that $p75^{NTR}$ was required for peri-infarct sympathetic denervation after ischemia-reperfusion. Numerous studies have shown that sympathetic denervation occurs both in the infarct and in the viable peri-infarct myocardium (Barber et al., 1983; Inoue and Zipes, 1987; Inoue and Zipes, 1988; Kammerling et al., 1987; Li et al., 2004; Minardo et al., 1988; Stanton et al., 1989). The loss of functional sympathetic fibers in the viable myocardium occurs minutes after ischemia (Inoue and Zipes, 1988) and can persist for years in humans (Stanton et al., 1989; Vaseghi et al., 2012). Two independent studies recently linked the amount of denervation detectable after MI to the probability of serious ventricular arrhythmias occurring in the years after the injury (Boogers et al., 2010; Nishisato et al., 2010). Although denervation of the infarct was not affected by the presence of $p75^{NTR}$, the loss of sympathetic fibers outside of the infarct was an active process that required $p75^{NTR}$. Thus, $p75^{NTR}$ might be an interesting target for pharmacological intervention, given the detrimental effects of denervation in human studies. The lack of p75 has little effect on cardiac function 3 days after MI (Lorentz et al., 2011), but it will be very interesting to determine if peri-infarct denervation increases arrhythmia susceptibility. $P75^{NTR-/-}$ hearts exhibit rhythm instability and high levels of spontaneous arrhythmias due to decreased innervation of the subendocardium (Lorentz *et al.*, 2010). Therefore, generation of an alternative model such as an inducible $p75^{NTR}$ knockout, will be needed to test if peri-infarct denervation contributes to arrhythmia generation.

Although $p75^{NTR}$ was required for peri-infarct denervation, it attenuated sympathetic hyperinnervation in distal peri-infarct areas. This is consistent with the observation that NGF

stimulates greater axon outgrowth in sympathetic neurons that lack $p75^{NTR}$ (Kohn et al., 1999; Lorentz et al., 2010). $P75^{NTR}$ can functionally antagonize downstream TrkA signaling (Hannila et al., 2004), and increased TrkA activation by NGF may explain the increased axonal elongation in $p75^{NTR-/-}$ hearts. However, NT-3 can also bind to and activate TrkA (Belliveau et al., 1997), and NT-3 activation of TrkA is significantly higher in the absence of $p75^{NTR}$ (Brennan et al., 1999). Therefore, the exacerbated hyperinnervation in $p75^{NTR-/-}$ mice could also be a result of neurons responding to both NGF and NT-3. Two lines of evidence suggest that NGF, rather than NT-3, is the main trigger for peri-infarct sympathetic regeneration. First, NT-3 mRNA is not increased in the myocardium after ischemia-reperfusion (Hiltunen et al., 2001). Second, infarct-induced nerve sprouting in sympathetic ganglion/heart co-cultures is blocked by anti-NGF antibodies (Gardner and Habecker, 2013; Hasan et al., 2006). This suggests that cardiac NGF is the primary stimulus for nerve regeneration in distal areas of peri-infarct myocardium.

Hyperinnervation was detected in both the left and right ventricles of $p75^{NTR-/-}$ hearts after myocardial infarction. The increase in sympathetic fiber density did not result in higher NE content in either the RV or the peri-infarct left ventricle (Lorentz et al., 2011), suggesting that additional factors are regulating NE synthesis, release, or reuptake. The dramatic depletion of NE in the peri-infarct left ventricle is caused by inflammatory cytokines stimulating local proteasomal degradation of TH (Shi and Habecker, 2012). Since the right ventricle is far removed from the damaged region of the left ventricle, it was surprising to detect changes in innervation density and NE content that were similar to the peri-infarct left ventricle. Inflammatory cells are an important source of NGF in the heart after MI (Hasan et al., 2006; Wernli et al., 2009), as well as releasing inflammatory cytokines. Although it remains unclear why NE levels are lower than expected in hyperinnervated left and right ventricle 3 days after myocardial infarction, it is likely that infiltrating immune cells play an important role.

A week after surgery peri-infarct innervation densities were not significantly different than control animals in either genotype, but fiber densities in the proximal peri-infarct region trended low in both genotypes. That was surprising in $p75^{NTR-/-}$ hearts, where proximal innervation density trended higher than shams 24 hours after MI. The recent discovery that the infarct is covered with chondroitin-sulfate proteoglycans that repel sympathetic axons (Gardner and Habecker, 2013) may explain the $p75^{NTR}$-independent decrease in fiber density adjacent to the infarct. Farther away from the infarct, areas of hyperinnervation also returned to control levels in WT and $p75^{NTR-/-}$ hearts, indicating that axon pruning in this context does not require $p75^{NTR}$. This is interesting, because activation of $p75^{NTR}$ together with differences in nerve activity has been implicated in sympathetic axon pruning during development (Singh et al., 2008). It is unlikely that decreased nerve activity plays a role in post-infarct pruning, given the chronic activation of cardiac sympathetic neurons after myocardial infarction (Dae et al., 1995; Du et al., 1999). However, several other factors that are responsible for axon retraction during development, including ephrins and semaphorins, are expressed in the heart (Ieda et al., 2007; Luo and O'Leary, 2005; Mansson-Broberg et al., 2008) and may play a role in pruning hyperinnervated regions after ischemia-reperfusion. Further studies will be required to elucidate the mechanisms of sympathetic pruning in the peri-infarct ventricle.

BDNF activation of $p75^{NTR}$ can induce axon degeneration in cultured sympathetic neurons (Singh et al., 2008), and BDNF mRNA is transiently elevated in myocytes at the infarct border zone 2–5 hours after ischemia- reperfusion (Hiltunen et al., 2001). We examined BDNF expression in the ventricle 24 hours after reperfusion using *Bdnf-HA* mice to circumvent issues with BDNF antibodies. We found HA-tagged BDNF localized to cells that resemble infiltrating immune cells rather than myocytes. Although we did not observe

BDNF protein at the border zone 24 hours after injury, there may be an early phase of BDNF expression in heart cells, followed by a later phase in which the source of BDNF is infiltrating immune cells. An additional $p75^{NTR}$ ligand, proNGF, is also elevated in the post-MI left ventricle (Siao et al., 2012). Although immunohistochemical analysis of BDNF-HA expression allowed us to localize the protein, it did not allow us to distinguish proBDNF and mature BDNF. Pro-neurotrophins preferentially bind $p75^{NTR}$ rather than TrkA on sympathetic neurons (Lee et al., 2001), making proNGF and proBDNF candidates for triggering $p75^{NTR}$-dependent axon degeneration. Thus, proNGF, BDNF, or proBDNF are all candidates to stimulate sympathetic denervation via $p75^{NTR}$.

In conclusion, we found that $p75^{NTR}$ stimulates peri-infarct sympathetic denervation but attenuates distal peri-infarct hyperinnervation. Pruning of hyperinnervated areas was not impaired by the absence of $p75^{NTR}$. We also found that a form of the $p75^{NTR}$ ligand BDNF (either pro or mature) is localized to the infarct 24 hours after myocardial infarction. The amount of sympathetic denervation after MI predicts the probability of serious ventricular arrhythmias in humans (Boogers et al., 2010; Nishisato et al., 2010), making $p75^{NTR}$ an interesting target for therapeutic intervention to prevent peri-infarct denervation.

Acknowledgments

Supported by AHA 0715669Z & 09PRE2110052 (C.U.L), AHA 0555553Z & NIH HL093056 (B.A.H.); OHSU Graduate Research Fellowship (DCP) and NIH NS030687, NS 064114 to BLH. The authors thank Cassandra Dunbar for technical assistance.

Abbreviations

BDNF	brain-derived neurotrophic factor
HA	hemagglutinin
123I-MIBG	iodine-123 meta-iodobenzylguanidine
LAD	left anterior descending coronary artery
MI	myocardial infarction
NGF	nerve growth factor
NE	norepinephrine
$P75^{NTR}$	p75 neurotrophin receptor
SCG	superior cervical ganglia
TrkA	tropomyosin-related receptor kinase A
TH	tyrosine hydroxylase

References

Abe T, Morgan DA, Gutterman DD. Protective role of nerve growth factor against postischemic dysfunction of sympathetic coronary innervation. Circulation. 1997; 95:213–220. [PubMed: 8994439]

Acheson AL, Naujoks K, Thoenen H. Nerve growth factor-mediated enzyme induction in primary cultures of bovine adrenal chromaffin cells: specificity and level of regulation. J Neurosci. 1984; 4:1771–1780. [PubMed: 6145760]

Al Shawi R, Hafner A, Chun S, Raza S, Crutcher K, Thrasivoulou C, Simons P, Cowen T. ProNGF, Sortilin, and Age-related Neurodegeneration. Ann N Y Acad Sci. 2007; 1119:208–215. [PubMed: 18056969]

Alston EN, Parrish DC, Hasan W, Tharp K, Pahlmeyer L, Habecker BA. Cardiac ischemia-reperfusion regulates sympathetic neuropeptide expression through gp130-dependent and independent mechanisms. Neuropeptides. 2011; 45:33–42. [PubMed: 21035185]

Barber MJ, Mueller TM, Henry DP, Felten SY, Zipes DP. Transmural myocardial infarction in the dog produces sympathectomy in noninfarcted myocardium. Circulation. 1983; 67:787–796. [PubMed: 6825234]

Belliveau DJ, Krivko I, Kohn J, Lachance C, Pozniak C, Rusakov D, Kaplan D, Miller FD. NGF and neurotrophin-3 both activate TrkA on sympathetic neurons but differentially regulate survival and neuritogenesis. J Cell Biol. 1997; 136:375–388. [PubMed: 9015308]

Boogers MJ, Borleffs CJ, Henneman MM, van Bommel RJ, van RJ, Boersma E, Dibbets-Schneider P, Stokkel MP, van der Wall EE, Schalij MJ, Bax JJ. Cardiac sympathetic denervation assessed with 123-iodine metaiodobenzylguanidine imaging predicts ventricular arrhythmias in implantable cardioverter-defibrillator patients. J Am Coll Cardiol. 2010; 55:2769–2777. [PubMed: 20538172]

Brennan C, Rivas-Plata K, Landis SC. The p75 neurotrophin receptor influences NT-3 responsiveness of sympathetic neurons in vivo. Nat Neurosci. 1999; 2:699–705. [PubMed: 10412058]

Cao JM, Chen LS, KenKnight BH, Ohara T, Lee MH, Tsai J, Lai WW, Karagueuzian HS, Wolf PL, Fishbein MC, Chen PS. Nerve sprouting and sudden cardiac death. Circ Res. 2000; 86:816–821. [PubMed: 10764417]

Crowley C, Spencer SD, Nishimura MC, Chen KS, Pitts-Meek S, Armaninl MP, Ling LH, McMahon SB, Shelton DL, Levinson AD, Phillips HS. Mice lacking nerve growth factor display perinatal loss of sensory and sympathetic neurons yet develop basal forebrain cholinergic neurons. Cell. 1994; 76:1001–1011. [PubMed: 8137419]

Dae MW, O'Connell JW, Botvinick EH, Chin MC. Acute and chronic effects of transient myocardial ischemia on sympathetic nerve activity, density, and norepinephrine content. Cardiovasc Res. 1995; 30:270–280. [PubMed: 7585815]

Deinhardt K, Kim T, Spellman DS, Mains RE, Eipper BA, Neubert TA, Chao MV, Hempstead BL. Neuronal growth cone retraction relies on proneurotrophin receptor signaling through Rac. Sci Signal. 2011; 4:ra82. [PubMed: 22155786]

Du XJ, Cox HS, Dart AM, Esler MD. Sympathetic activation triggers ventricular arrhythmias in rat heart with chronic infarction and failure. Cardiovasc Res. 1999; 43:919–929. [PubMed: 10615419]

Gardner RT, Habecker BA. Infarct-derived chondroitin sulfate proteoglycans prevent sympathetic reinnervation after cardiac ischemia-reperfusion injury. J Neurosci. 2013; 33:7175–7183. [PubMed: 23616527]

Glebova NO, Ginty DD. Heterogeneous Requirement of NGF for Sympathetic Target Innervation In Vivo. J Neurosci. 2004; 24:743–751. [PubMed: 14736860]

Habecker BA, Bilimoria P, Linick C, Gritman K, Lorentz CU, Woodward W, Birren SJ. Regulation of cardiac innervation and function via the p75 neurotrophin receptor. Auton Neurosci. 2008; 140:40–48. [PubMed: 18430612]

Hannila SS, Lawrance GM, Ross GM, Kawaja MD. TrkA and mitogen-activated protein kinase phosphorylation are enhanced in sympathetic neurons lacking functional p75 neurotrophin receptor expression. Eur J Neurosci. 2004; 19:2903–2908. [PubMed: 15147324]

Hasan W, Jama A, Donohue T, Wernli G, Onyszchuk G, Al Hafez B, Bilgen M, Smith PG. Sympathetic hyperinnervation and inflammatory cell NGF synthesis following myocardial infarction in rats. Brain Res. 2006; 1124:142–154. [PubMed: 17084822]

Hassankhani A, Steinhelper ME, Soonpaa MH, Katz EB, Taylor DA, Andrade-Rozental A, Factor SM, Steinberg JJ, Field LJ, Federoff HJ. Overexpression of NGF within the heart of transgenic mice causes hyperinnervation, cardiac enlargement, and hyperplasia of ectopic cells. Dev Biol. 1995; 169:309–321. [PubMed: 7750647]

Hiltunen JO, Laurikainen A, Vakeva A, Meri S, Saarma M. Nerve growth factor and brain-derived neurotrophic factor mRNAs are regulated in distinct cell populations of rat heart after ischaemia and reperfusion. J Pathol. 2001; 194:247–253. [PubMed: 11400155]

Ieda M, Kanazawa H, Kimura K, Hattori F, Ieda Y, Taniguchi M, Lee JK, Matsumura K, Tomita Y, Miyoshi S, Shimoda K, Makino S, Sano M, Kodama I, Ogawa S, Fukuda K. Sema3a maintains

normal heart rhythm through sympathetic innervation patterning. Nat Med. 2007; 13:604–612. [PubMed: 17417650]

Inoue H, Zipes DP. Results of sympathetic denervation in the canine heart: supersensitivity that may be arrhythmogenic. Circulation. 1987; 75:877–887. [PubMed: 3829345]

Inoue H, Zipes DP. Time course of denervation of efferent sympathetic and vagal nerves after occlusion of the coronary artery in the canine heart. Circ Res. 1988; 62:1111–1120. [PubMed: 3383360]

Kammerling JJ, Green FJ, Watanabe AM, Inoue H, Barber MJ, Henry DP, Zipes DP. Denervation supersensitivity of refractoriness in noninfarcted areas apical to transmural myocardial infarction. Circulation. 1987; 76:383–393. [PubMed: 3038369]

Kohn J, Aloyz RS, Toma JG, Haak-Frendscho M, Miller FD. Functionally antagonistic interactions between the TrkA and p75 neurotrophin receptors regulate sympathetic neuron growth and target innervation. J Neurosci. 1999; 19:5393–5408. [PubMed: 10377349]

Krizsan-Agbas D, Pedchenko T, Hasan W, Smith PG. Oestrogen regulates sympathetic neurite outgrowth by modulating brain derived neurotrophic factor synthesis and release by the rodent uterus. Eur J Neurosci. 2003; 18:2760–2768. [PubMed: 14656325]

Lee KF, Li E, Huber LJ, Landis SC, Sharpe AH, Chao MV, Jaenisch R. Targeted mutation of the gene encoding the low affinity NGF receptor p75 leads to deficits in the peripheral sensory nervous system. Cell. 1992; 69:737–749. [PubMed: 1317267]

Lee R, Kermani P, Teng KK, Hempstead BL. Regulation of cell survival by secreted proneurotrophins. Science. 2001; 294:1945–1948. [PubMed: 11729324]

Li W, Knowlton D, Van Winkle DM, Habecker BA. Infarction alters both the distribution and noradrenergic properties of cardiac sympathetic neurons. Am J Physiol Heart Circ Physiol. 2004; 286:H2229–H2236. [PubMed: 14726300]

Lorentz CU, Alston EN, Belcik JT, Lindner JR, Giraud GD, Habecker BA. Heterogeneous ventricular sympathetic innervation, altered {beta} adrenergic receptor expression, and rhythm instability in mice lacking p75 neurotrophin receptor. Am J Physiol Heart Circ Physiol. 2010; 298:H1652–H1660. [PubMed: 20190098]

Lorentz CU, Woodward WR, Tharp K, Habecker BA. Altered norepinephrine content and ventricular function in p75NTR−/− mice after myocardial infarction. Auton Neurosci. 2011; 164:13–19. [PubMed: 21646052]

Luo L, O'Leary DDM. Axon retraction and degeneration in development and disease. Annual Review of Neuroscience. 2005; 28:127–156.

Mansson-Broberg A, Siddiqui AJ, Genander M, Grinnemo KH, Hao X, Andersson AB, Wardell E, Sylven C, Corbascio M. Modulation of ephrinB2 leads to increased angiogenesis in ischemic myocardium and endothelial cell proliferation. Biochem Biophys Res Commun. 2008; 373:355–359. [PubMed: 18571496]

Meloni M, Caporali A, Graiani G, Lagrasta C, Katare R, Van LS, Spillmann F, Campesi I, Madeddu P, Quaini F, Emanueli C. Nerve Growth Factor Promotes Cardiac Repair following Myocardial Infarction. Circ Res. 2010; 106:1275–1284. [PubMed: 20360245]

Minardo JD, Tuli MM, Mock BH, Weiner RE, Pride HP, Wellman HN, Zipes DP. Scintigraphic and electrophysiological evidence of canine myocardial sympathetic denervation and reinnervation produced by myocardial infarction or phenol application. Circulation. 1988; 78:1008–1019. [PubMed: 3168182]

Nademanee K, Taylor R, Bailey WE, Rieders DE, Kosar EM. Treating electrical storm: sympathetic blockade versus advanced cardiac life support-guided therapy. Circulation. 2000; 102:742–747. [PubMed: 10942741]

Naujoks KW, Korsching S, Rohrer H, Thoenen H. Nerve growth factor-mediated induction of tyrosine hydroxylase and of neurite outgrowth in cultures of bovine adrenal chromaffin cells: dependence on developmental stage. Dev Biol. 1982; 92:365–379. [PubMed: 6126414]

Nishisato K, Hashimoto A, Nakata T, Doi T, Yamamoto H, Nagahara D, Shimoshige S, Yuda S, Tsuchihashi K, Shimamoto K. Impaired Cardiac Sympathetic Innervation and Myocardial Perfusion Are Related to Lethal Arrhythmia: Quantification of Cardiac Tracers in Patients with ICDs. J Nucl Med. 2010; 51:1241–1249. [PubMed: 20679471]

Nykjaer A, Lee R, Teng KK, Jansen P, Madsen P, Nielsen MS, Jacobsen C, Kliemannel M, Schwarz E, Willnow TE, Hempstead BL, Petersen CM. Sortilin is essential for proNGF-induced neuronal cell death. Nature. 2004; 427:843–848. [PubMed: 14985763]

Oh YS, Jong AY, Kim DT, Li H, Wang C, Zemljic-Harpf A, Ross RS, Fishbein MC, Chen PS, Chen LS. Spatial distribution of nerve sprouting after myocardial infarction in mice. Heart Rhythm. 2006; 3:728–736. [PubMed: 16731479]

Otten U, Schwab M, Gagnon C, Thoenen H. Selective induction of tyrosine hydroxylase and dopamine beta-hydroxylase by nerve growth factor: comparison between adrenal medulla and sympathetic ganglia of adult and newborn rats. Brain Res. 1977; 133:291–303. [PubMed: 20194]

Parrish DC, Alston EN, Rohrer H, Hermes SM, Aicher SA, Nkadi P, Woodward WR, Stubbusch J, Gardner RT, Habecker BA. The absence of gp130 in dopamine {beta} hydroxylase-expressing neurons leads to autonomic imbalance and increased reperfusion arrhythmias. Am J Physiol Heart Circ Physiol. 2009a; 297:H960–H967. [PubMed: 19592611]

Parrish DC, Alston EN, Rohrer H, Nkadi P, Woodward WR, Schutz G, Habecker BA. Infarction-induced cytokines cause local depletion of tyrosine hydroxylase in cardiac sympathetic nerves. Exp Physiol. 2009b; 95:304–314. [PubMed: 19880537]

Pellegrino MJ, Parrish DC, Zigmond RE, Habecker BA. Cytokines inhibit norepinephrine transporter expression by decreasing Hand2. Mol Cell Neurosci. 2011; 46:671–680. [PubMed: 21241805]

Rubart M, Zipes DP. Mechanisms of sudden cardiac death. J Clin Invest. 2005; 115:2305–2315. [PubMed: 16138184]

Scherrer-Crosbie M, Mardon K, Cayla J, Syrota A, Merlet P. Alterations of myocardial sympathetic innervation in response to hypoxia. J Nucl Med. 1997; 38:954–957. [PubMed: 9189149]

Shi X, Habecker BA. gp130 cytokines stimulate proteasomal degradation of tyrosine hydroxylase via extracellular signal regulated kinases 1 and 2. J Neurochem. 2012; 120:239–247. [PubMed: 22007720]

Shi X, Woodward WR, Habecker BA. Ciliary neurotrophic factor stimulates tyrosine hydroxylase activity. J Neurochem. 2012; 121:700–704. [PubMed: 22372951]

Siao CJ, Lorentz CU, Kermani P, Marinic T, Carter J, McGrath K, Padow VA, Mark W, Falcone DJ, Cohen-Gould L, Parrish DC, Habecker BA, Nykjaer A, Ellenson LH, Tessarollo L, Hempstead BL. ProNGF, a cytokine induced after myocardial infarction in humans, targets pericytes to promote microvascular damage and activation. J Exp Med. 2012; 209:2291–2305. [PubMed: 23091165]

Singh KK, Park KJ, Hong EJ, Kramer BM, Greenberg ME, Kaplan DR, Miller FD. Developmental axon pruning mediated by BDNF-p75NTR-dependent axon degeneration. Nat Neurosci. 2008; 11:649–658. [PubMed: 18382462]

Smeyne RJ, Klein R, Schnapp A, Long LK, Bryant S, Lewin A, Lira SA, Barbacid M. Severe sensory and sympathetic neuropathies in mice carrying a disrupted Trk/NGF receptor gene. Nature. 1994; 368:246–249. [PubMed: 8145823]

Solomon SD, Zelenkofske S, McMurray JJ, Finn PV, Velazquez E, Ertl G, Harsanyi A, Rouleau JL, Maggioni A, Kober L, White H, Van de WF, Pieper K, Califf RM, Pfeffer MA. Sudden death in patients with myocardial infarction and left ventricular dysfunction, heart failure, or both. N Engl J Med. 2005; 352:2581–2588. [PubMed: 15972864]

Stanton MS, Tuli MM, Radtke NL, Heger JJ, Miles WM, Mock BH, Burt RW, Wellman HN, Zipes DP. Regional sympathetic denervation after myocardial infarction in humans detected noninvasively using I-123-metaiodobenzylguanidine. J Am Coll Cardiol. 1989; 14:1519–1526. [PubMed: 2809013]

Thoenen H, Angeletti PU, Levi-Montalcini R, Kettler R. Selective induction by nerve growth factor of tyrosine hydroxylase and dopamine-β-hydroxylase in the rat superior cervical ganglia. Proc Natl Acad Sci U S A. 1971; 68:1598–1602. [PubMed: 5283951]

Vaseghi M, Lux RL, Mahajan A, Shivkumar K. Sympathetic stimulation increases dispersion of repolarization in humans with myocardial infarction. Am J Physiol Heart Circ Physiol. 2012

Wernli G, Hasan W, Bhattacherjee A, van RN, Smith PG. Macrophage depletion suppresses sympathetic hyperinnervation following myocardial infarction. Basic Res Cardiol. 2009; 104:681–693. [PubMed: 19437062]

Yamamori T, Fukada K, Aebersold R, Korsching S, Fann MJ, Patterson PH. The cholinergic neuronal differentiation factor from heart cells is identical to leukemia inhibitory factor. Science. 1989; 246:1412–1416. [PubMed: 2512641]

Yang J, Siao CJ, Nagappan G, Marinic T, Jing D, McGrath K, Chen ZY, Mark W, Tessarollo L, Lee FS, Lu B, Hempstead BL. Neuronal release of proBDNF. Nat Neurosci. 2009; 12:113–115. [PubMed: 19136973]

Zhou S, Chen LS, Miyauchi Y, Miyauchi M, Kar S, Kangavari S, Fishbein MC, Sharifi B, Chen PS. Mechanisms of cardiac nerve sprouting after myocardial infarction in dogs. Circ Res. 2004; 95:76–83. [PubMed: 15166093]

Highlights

- $p75^{NTR}$ is required for peri-infarct sympathetic denervation after MI
- $p75^{NTR}$ inhibits peri-infarct sympathetic nerve sprouting after MI
- $p75^{NTR}$ has no effect on pruning in hyperinnervated regions after MI
- A form of the $p75^{NTR}$ ligand BDNF is localized to the infarct after MI

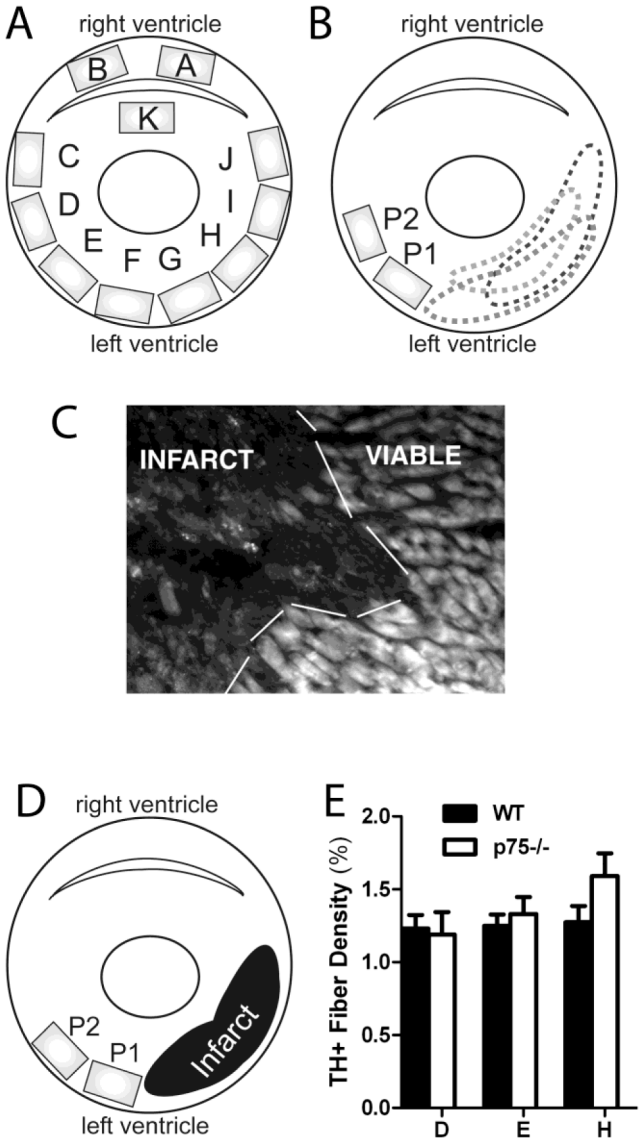

Figure 1.

Method for quantification of sympathetic innervation. A) Cartoon cross section of the left and right ventricles showing the 11 fields of view analyzed (A–K). Pictures A and B were taken from the right ventricle, C–J were taken from the subepicardium of the left ventricle, and K was taken from the septum. B) Cartoon cross section of the left and right ventricles showing the variable location of the infarct after ischemia-reperfusion. The proximal peri-infarct region (P1) was defined as the field of view adjacent to the infarct and the distal peri-infarct region (P2) was defined as the field of view adjacent to P1 (530 μm from the infarct). C) Photomicrograph depicting the infarct 7 days after ischemia-reperfusion and the adjacent viable myocardium. D) Cartoon cross section of the regions quantified. One representative picture within the infarct was averaged over the four sections analyzed. E) Quantification of sympathetic fiber density in sham-operated animals from WT (black bars) and $p75^{NTR-/-}$ mice (white bars) from three fields of view (D, E, and H) that correspond to P2, P1, and infarct regions after MI respectively, mean ± SEM, n=8.

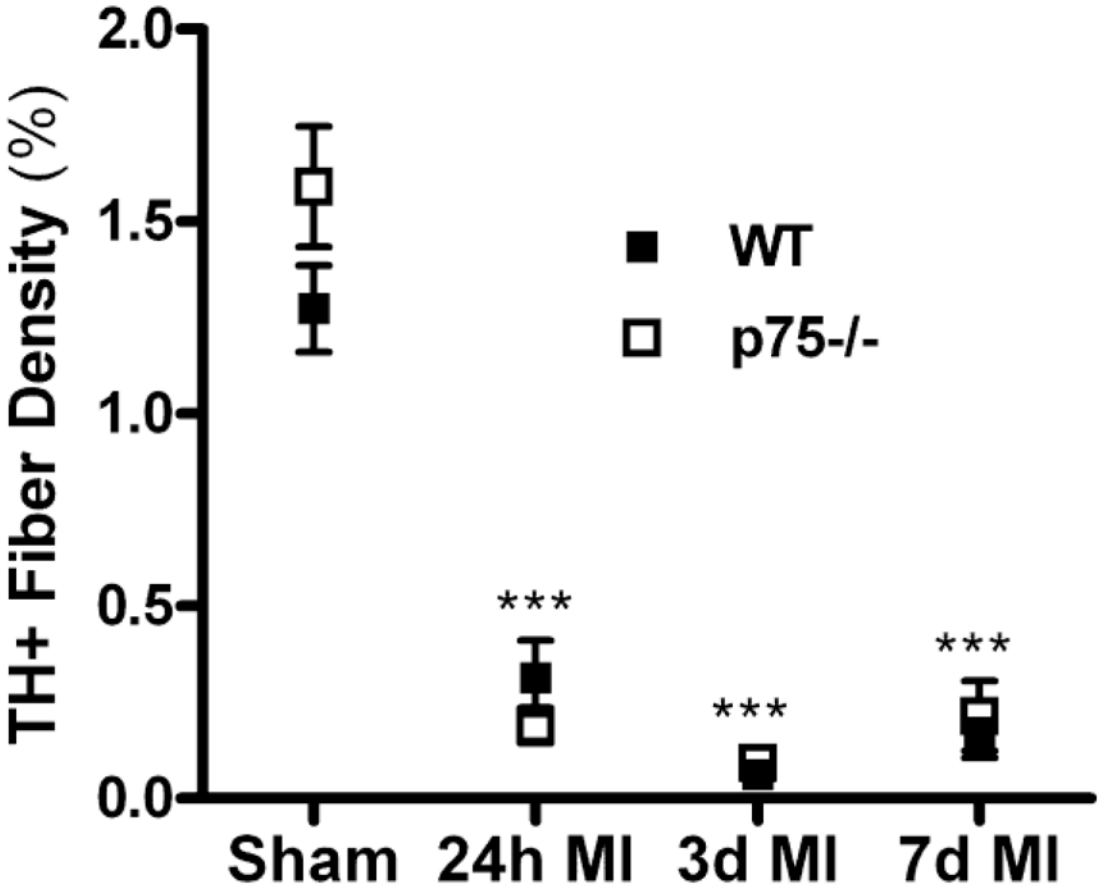

Figure 2.

Sympathetic denervation occurs in the infarct after ischemia-reperfusion. Quantification of sympathetic fiber density in the infarct 24 hours, 3 days, and 7 days after ischemia-reperfusion from WT (black squares) and $p75^{NTR-/-}$ mice (open squares) compared to sham operated animals, mean ± SEM, ***p< 0.001, n=4 (24 hrs) or n=6–8 (sham, 3 day, 7 day).

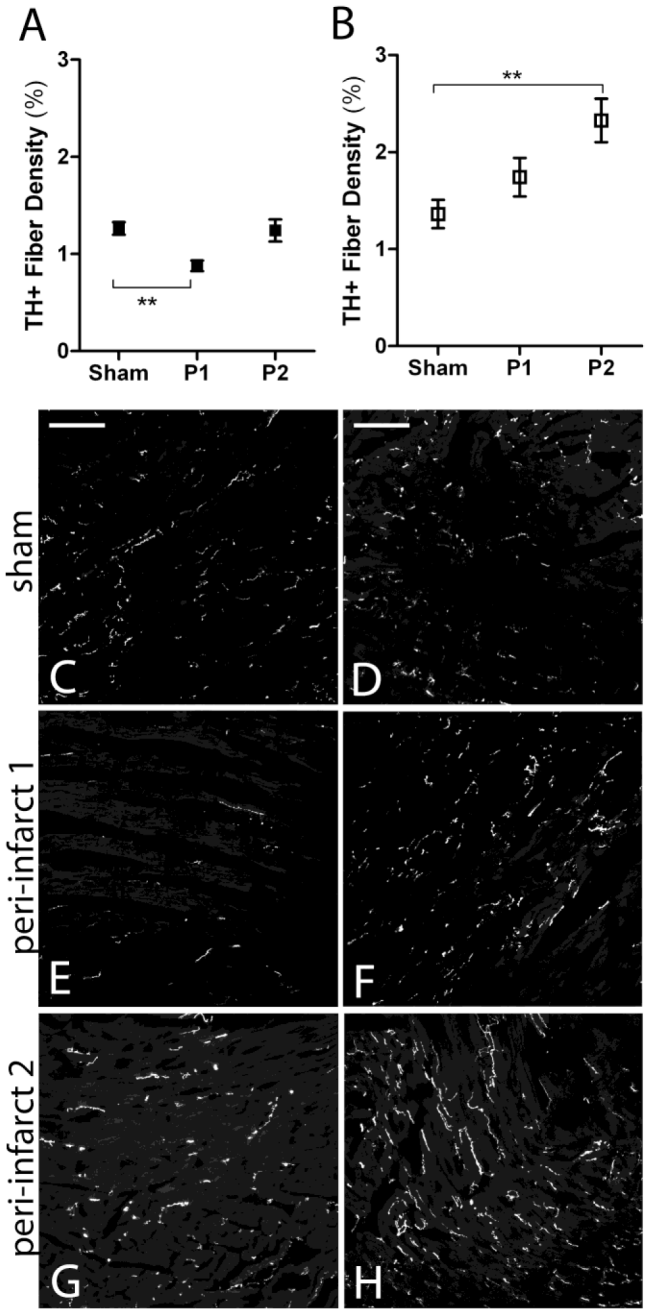

Figure 3.

Sympathetic innervation density 24 hours after ischemia-reperfusion in WT and $p75^{NTR-/-}$ peri-infarct left ventricle. A) Quantification of sympathetic fiber density in the proximal peri-infarct region (P1) and distal peri-infarct region (P2) 24 hours after ischemia-reperfusion from WT (black squares) and B) $p75^{NTR-/-}$ mice (open squares), mean ± SEM, *p< 0.05, n=4–8. C) Representative picture from WT sham operated left ventricle D) and from $p75^{NTR-/-}$ left ventricle. E) Representative picture from the proximal peri-infarct region (peri-infarct 1, P1) from WT mice and F) from $p75^{NTR-/-}$ mice. G) Representative picture from the distal peri-infarct region (peri-infarct 2, P2) from WT mice and H) $p75^{NTR-/-}$ mice. Scale bars= 100μm

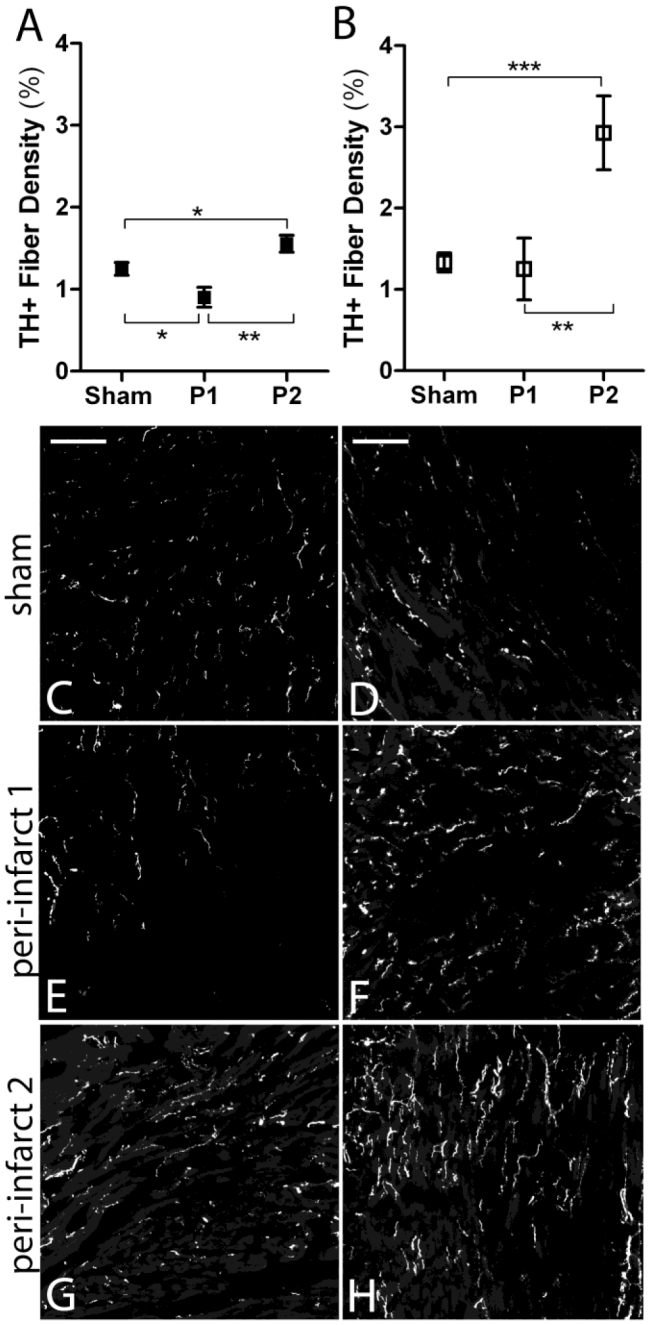

Figure 4.

Sympathetic innervation density 3 days after ischemia-reperfusion in WT and $p75^{NTR-/-}$ peri-infarct left ventricle. A) Quantification of sympathetic fiber density in the proximal peri-infarct region (P1) and distal peri-infarct region (P2) 3 days after ischemia-reperfusion from WT (black squares) and B) $p75^{NTR-/-}$ mice (open squares), mean ± SEM, *p< 0.05, **p< 0.01, ***p< 0.001, n=6–8. C) Representative picture from WT sham operated left ventricle D) and from $p75^{NTR-/-}$ left ventricle. E) Representative picture from the proximal peri-infarct region (peri-infarct 1, P1) 3 days after ischemia-reperfusion from WT mice and F) from $p75^{NTR-/-}$ mice. G) Representative picture from the distal peri-infarct region (peri-

infarct 2, P2) 3 days after ischemia-reperfusion from WT mice and H) $p75^{NTR-/-}$ mice. Scale bars= 100μm

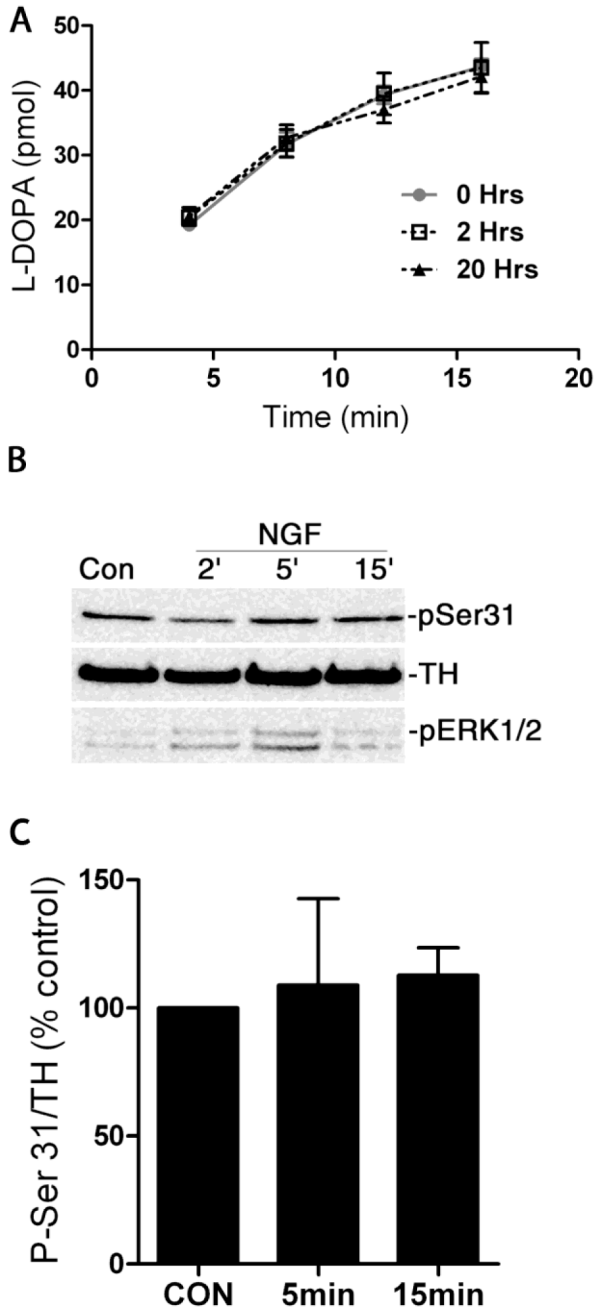

Figure 5. NGF does not stimulate TH activity

A) Sympathetic neurons were treated with NGF (100ng/ml) for 2 or 20hrs and TH activity was assessed by quantifying the rate of L-DOPA production. This graph shows a representative experiment done in quadruplicate. Since TH protein levels did not differ significantly between replicates or treatment groups, the data are expressed as the amount of L-DOPA produced over time. B) Dissociated sympathetic neurons were treated with NGF (100ng/ml) for 2, 5, and 15 minutes, and blotted for phosphorylated (pSer31) and total (TH) tyrosine hydroxylase. Phospho-ERK1/2 (pERK1/2) was a positive control for NGF stimulation. C) Quantification of phospho-Ser31 TH relative to total TH. Data are calculated as percent of control and averaged across 3 independent experiments (mean ± SEM).

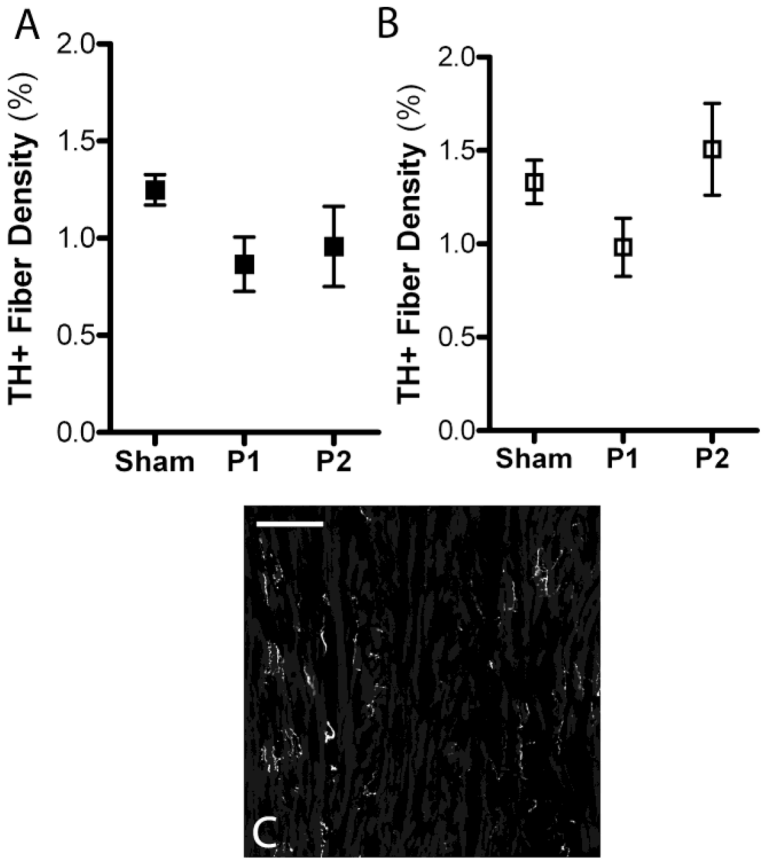

Figure 6.

Sympathetic innervation density 7 days after ischemia-reperfusion in WT and *p75*$^{NTR-/-}$ peri-infarct left ventricle. A) Quantification of sympathetic fiber density in the proximal peri-infarct region (P1) and distal peri-infarct region (P2) 7 days after ischemia-reperfusion from WT (black squares) and B) *p75*$^{NTR-/-}$ mice (open squares), mean ± SEM, n=6–8. C) Representative picture from WT peri-infarct region 7 days after ischemia-reperfusion shows heterogeneous sympathetic innervation with distinct regions of denervated myocardium next hyperinnervated regions, scale bar= 100μm.

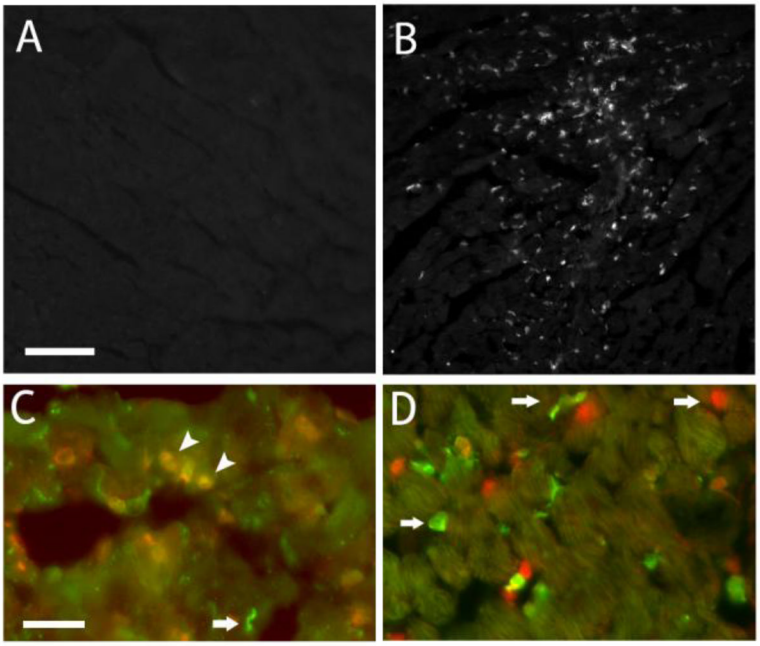

Figure 7.

BDNF protein is elevated in the left ventricle 24 hours after ischemia-reperfusion. Representative pictures of immunofluorescence detection of BDNF using an antibody to HA in the left ventricle from *Bdnf-HA* mice 24 hrs after sham surgery (A) or ischemia-reperfusion (B), scale bar A, B= 100μm. C, D) Co-immunofluorescence detection of BDNF-HA (green), and in red the neutrophil marker Ly-6B.2 (C) or macrophage marker Mac2 (D). Scale bar C, D= 25μm. Arrows highlight cells labeled for a single marker and arrowheads highlight neutrophils positive for both HA and Ly-6B.2.

Table 1

Ventricular Sympathetic Innervation Density

Region	WT 3d MI (n=6)	WT 7d MI (n=7)
A	118.5 ± 50.6	56.7 ± 31.2 *
B	106.1 ± 69.2	65.1 ± 46.1
C	111.7 ± 36.5	91.4 ± 42.9
D	84.8 ± 31.8	71.1 ± 34.0
E	72.8 ± 26.5	68.7 ± 48.4
F	57.8 ± 35.6 *	73.2 ± 38.6
G	33.1 ± 21.1 ***	53.4 ± 29.9 **
H	9.2 ± 12.7 ***	30.6 ± 36.1 ***
I	8.3 ± 8.4 ***	12.7 ± 16.9 ***
J	41.3 ± 36.1 *	17.9 ± 21.6 **
K	87.7 ± 28.4	93.4 ± 53.4

Values are % sham operated control, mean ± SD.